npg

ORIGINAL ARTICLE

NF-κB1 p105 suppresses lung tumorigenesis through the Tpl2 kinase but independently of its NF-κB function

F Sun[1,2], Z Qu[1,2], Y Xiao[1,3], J Zhou[1,2], TF Burns[1], LP Stabile[1,4], JM Siegfried[1,4,5] and G Xiao[1,2]

Nuclear factor-κB (NF-κB) is generally believed to be pro-tumorigenic. Here we report a tumor-suppressive function for NF-κB1, the prototypical member of NF-κB. While NF-κB1 downregulation is associated with high lung cancer risk in humans and poor patient survival, NF-κB1-deficient mice are more vulnerable to lung tumorigenesis induced by the smoke carcinogen, urethane. Notably, the tumor-suppressive function of NF-κB1 is independent of its classical role as an NF-κB factor, but instead through stabilization of the Tpl2 kinase. NF-κB1-deficient tumors exhibit 'normal' NF-κB activity, but a decreased protein level of Tpl2. Reconstitution of Tpl2 or the NF-κB1 p105, but not p50 (the processed product of p105), inhibits the tumorigenicity of NF-κB1-deficient lung tumor cells. Remarkably, Tpl2-knockout mice resemble NF-κB1 knockouts in urethane-induced lung tumorigenesis. Mechanistic studies indicate that p105/Tpl2 signaling is required for suppressing urethane-induced lung damage and inflammation, and activating mutations of the K-Ras oncogene. These studies reveal an unexpected, NF-κB-independent but Tpl2-depednednt role of NF-κB1 in lung tumor suppression. These studies also reveal a previously unexplored role of p105/Tpl2 signaling in lung homeostasis.

Oncogene (2016) 35, 2299–2310; doi:10.1038/onc.2015.299; published online 24 August 2015

INTRODUCTION

Nuclear factor-κB (NF-κB) is not a single protein, but a collection of five structurally related inducible transcription factors that are able to bind to κB site-containing promoters to regulate gene expression.[1] Upon the molecular identification in 1990 of NF-κB1 and RelA (also known as p65), two prototypical members of NF-κB, as the homologs of the avian retroviral oncoprotein v-Rel, a role for NF-κB in tumorigenesis was highly expected.[2] Since then, the importance of NF-κB in tumor biology has been extensively investigated and is now widely appreciated.[1–3] Although oncogenic NF-κB mutations are relatively rare and mainly occur in certain hematological malignancies, constitutive activation of NF-κB has been detected in almost all tumors, either hematological or solid.[4,5] More importantly, aberrant NF-κB activation has been suggested to be involved in all steps of tumor development, from initiation to promotion, to progression, as well as resistance to cancer therapies.[1,3] Mechanistic studies indicate that NF-κB contributes to tumor pathogenesis both intrinsically and extrinsically. Within precancerous or cancerous cells, activated NF-κB induces a large range of genes not only to promote malignant cell survival, proliferation and metastasis but also to induce angiogenesis and tumorigenic inflammation.[1,3] Moreover, NF-κB activated in nontumor cells, in particular immune cells, also contributes to tumor pathogenesis indirectly through establishing a tumorigenic microenvironment.[1,3]

Intriguingly, the link between NF-κB and lung cancer has been established only quite recently, although lung cancer is the leading cause of cancer deaths worldwide.[6–9] NF-κB can be activated by tobacco smoking, the major risk factor that accounts for ~87% of lung cancer cases.[10,11] Accordingly, NF-κB is persistently activated in human lung cancers and aberrant NF-κB activation is associated with lung tumor progression and poor patient survival.[12] In-vitro cell line and in-vivo animal studies involving NF-κB inhibition suggest that persistent NF-κB activation is one important mechanism underlying lung cancer development and therapy resistance.[13–17]

Those studies, however, mainly focus on RelA and their conclusions on the tumorigenic role of NF-κB in lung and other cancers are largely derived from the anti-tumor effects of NF-κB inhibition by knockout/knockdown of the NF-κB activator IKK, overexpression of the NF-κB inhibitor IκBα or administration of IKK inhibitors.[12–17] IKK and IκBα have many NF-κB-independent functions that are also implicated in tumorigenesis.[18,19] Furthermore, they control the activation of other members of the NF-κB family, besides RelA.[1] Currently, it remains largely unknown whether and how individual NF-κB members are involved in lung and other cancers. Given the functional complexities of NF-κB members, addressing this question is of importance. It will not only advance our understanding of NF-κB's role in tumorigenesis but also set up a basis for us to target NF-κB for cancer therapy. This is particularly true for NF-κB1. NF-κB1 protein exists as two forms, p105 and p50, the precursor and mature forms, respectively.[1] NF-κB1 p50 is believed to be the most important functional partner of RelA and the RelA/p50 heterodimer is often referred to as NF-κB. On the other hand, NF-κB1 p105 has two different functions related to NF-κB: serving as an inhibitor of NF-κB and the precursor of p50.[1] In addition, NF-κB1 p105 also has an NF-κB-independent function: binding to and stabilizing Tpl2 (also known as Cot), a kinase that was originally identified as a proto-oncoprotein.[20,21]

[1]University of Pittsburgh Cancer Institute, University of Pittsburgh School of Medicine, Pittsburgh, PA, USA; [2]Department of Microbiology and Molecular Genetics, Hillman Cancer Center Research Pavilion, University of Pittsburgh School of Medicine, Pittsburgh, PA, USA; [3]Program of Biological Science, La Roche College, Pittsburgh, PA, USA and [4]Department of Pharmacology and Chemical Biology, University of Pittsburgh School of Medicine, Pittsburgh, PA, USA. Correspondence: Dr Z Qu, Hillman Cancer Center Research Pavilion, Room 1.18, 5117 Centre Avenue, Pittsburgh, PA 15213, USA or Dr G Xiao, Department of Microbiology and Molecular Genetics, Hillman Cancer Center Research Pavilion, University of Pittsburgh School of Medicine, 5117 Centre Avenue, Room 1.19, Pittsburgh, PA 15213, USA.
E-mail: quz@upmc.edu or xiaog2@upmc.edu
[5]Current address: Department of Pharmacology, University of Minnesota, Minneapolis, MN 55455, USA.
Received 29 October 2014; revised 4 June 2015; accepted 6 July 2015; published online 24 August 2015

Using lung cancer as a model, here we demonstrate an unexpected tumor-suppressive function for NF-κB1. Remarkably, NF-κB1 suppresses lung tumorigenesis independently of its NF-κB function but instead through p105 stabilization of Tpl2. The noncanonical p105/Tpl2 signaling pathway is required for maintaining pulmonary homeostasis under inflammation and oncogenic stress. Genetic deficiency of either p105 or Tpl2 makes animals susceptible to lung damage and inflammation, activating mutation of the K-Ras oncogene, and subsequent lung carcinogenesis in response to tobacco carcinogens. In addition to advancing our understanding of lung cancer and the complex functions of NF-κB1, these studies provide the first line of evidence demonstrating that the Tpl2 proto-oncoprotein may exert a tumor-suppressive effect.

RESULTS

Repression of NF-κB1 expression is involved in human lung cancer

Although recent studies have suggested RelA as a promoter of lung cancer, the potential roles of other members of the NF-κB family in this deadliest form of human cancer have not yet been examined. To address this important issue, we initially examined the expression levels of NF-κB1, the most important functional partner of RelA, in a large range of human lung cancer cell lines. Surprisingly, most human lung cancer cell lines we examined expressed significantly lower levels of NF-κB1 mRNA, in comparison with the normal human lung epithelial cell line NL-20 (Figure 1a). In line with the decreased mRNA expression, the protein levels of both NF-κB1 p105 and p50 were significantly lower in those human lung cancer cell lines (Figure 1b and Supplementary Figure S1). For simplicity, hereinafter, these cells are referred to as NF-κB1[low] lung cancer cells.

To test the clinical relevance of this finding, we examined the mRNA expression levels of NF-κB1 in human lung tumor tissues freshly isolated from patients and their matched normal control tissues from the same patients. Indeed, the mRNA expression level of NF-κB1 was significantly decreased in human primary lung tumor samples compared with their matched normal controls (Figure 1c). Immunohistochemistry (IHC) staining using an antibody that can recognize both p105 and p50 proteins indicating the protein expression of NF-κB1 was also repressed in human primary lung cancer tissues (Figure 1d). Our gene array analysis further indicated that the downregulation of NF-κB1 is associated with high risk of lung cancer in humans and poor patient survival (Figures 1e and f). These studies suggested that NF-κB1 repression is a clinically relevant event of human lung cancer.

To directly examine whether the repression of NF-κB1 expression contributes to the pathogenesis of human lung cancer, we reconstituted NF-κB1 cDNA, which expresses both p105 and p50 proteins, into NF-κB1[low] lung cancer cells (Figure 1g). Interestingly, NF-κB1 reconstitution alone was sufficient to block the growth of those NF-κB1[low] lung cancer cells in culture (Figure 1h). Moreover, NF-κB1 reconstitution also suppressed the anchorage-independent growth of those cancer cells (Figure 1i). On the other hand, further knockdown of NF-κB1 increased the growth of those cancer cells (Supplementary Figure S2). These data suggested that NF-κB1 downregulation is one important mechanism underlying human lung cancer pathogenesis.

NF-κB1-knockout mice are prone to lung tumorigenesis induced by the smoke carcinogen urethane

To systemically investigate the role of NF-κB1 repression in lung cancer, we employed a well-accepted and widely used mouse model of lung cancer induced by the tobacco carcinogen urethane. Urethane alone is sufficient to induce lung carcinogenesis in mice and, importantly, urethane-induced lung cancers in mice faithfully recapitulate human lung cancers, and in particular adenocarcinomas associated with tobacco smoking.[22] We initially examined whether NF-κB1 deficiency in mice makes animals more sensitive to urethane-induced lung tumorigenesis.

Consistent with previous findings that NF-κB1 is dispensable for lung development and function,[23] NF-κB1-knockout (NF-κB1[Δ/Δ]) mice did not show apparent abnormalities in lung size or morphology (Figure 2a and data not shown). Notably, NF-κB1[Δ/Δ] mice developed significantly more lung tumors than wild-type (WT) mice after exposure to urethane (Figures 2a and b). Moreover, the tumors in NF-κB1[Δ/Δ] mice were bigger than those in WT mice, as evidenced by a significant increase in the average size of tumors (Figure 2c). Consistent with this observation, both bromodeoxyuridine (BrdU) and Ki-67 proliferation assays showed that in comparison with WT tumors, NF-κB1[Δ/Δ] tumors showed an increased cell proliferation rate (Figures 2d and e). Of note, the absence of NF-κB1 in the tumors from urethane-treated NF-κB1[Δ/Δ] mice was validated by IHC and immunoblotting assays (Figure 2f). Our histology assays also showed that NF-κB1[Δ/Δ] mice had significantly more atypical adenomatous hyperplasia, adenomas and adenocarcinomas in their lungs (Supplementary Figure S3). These data clearly indicated that NF-κB1 deficiency contributes to both lung tumor development and progression in a urethane-induced lung tumor model.

Increased lung tumorigenesis in urethane-treated NF-κB1-knockout mice is associated with augmented lung damage, pro-tumorigenic inflammation and oncogenic K-Ras mutation

To investigate the mechanisms underlying the increased lung tumorigenesis in NF-κB1[Δ/Δ] mice, we examined the pulmonary inflammatory responses to urethane in NF-κB1[Δ/Δ] mice and WT mice, because recent studies indicated that pulmonary inflammation has a critical role in the initiation and progression of lung cancer.[24,25] Interestingly, we found that several pro-inflammatory cytokines that can promote tumor initiation and progression, such as tumor necrosis factor-α, interleukin-1β and interleukin-6, were significantly higher in the lungs of NF-κB1[Δ/Δ] mice compared with WT mice (Figure 3a). In addition, the immune cell-attractive chemokines CCL2, CCL3, CCL4 and CXCL2 were also significantly increased in the lungs of urethane-treated NF-κB1[Δ/Δ] mice (Figure 3a). Consistently, significantly more immune cells were represented in bronchoalveolar lavage fluid (BALF) from NF-κB1[Δ/Δ] mice (Figure 3b). Further analysis indicated that lymphocytes and macrophages were increased in the BALF of NF-κB1[Δ/Δ] mice. These data suggested that NF-κB1 restricts urethane-induced pro-tumorigenic inflammation.

In association with the increased pulmonary inflammation in urethane-treated NF-κB1[Δ/Δ] mice, much more serious lung injury was observed in these mice (Figure 3c). Before urethane treatment, the lungs of NF-κB1[Δ/Δ] mice were normal and displayed the same morphology and histology as those of WT mice (data not shown). However, exposure to urethane caused significantly enhanced alveolar thickening and congestion, loss of integrity of the alveolar capillary membrane, as well as perivascular edema and hemorrhage, leading to air space enlargement, protein leak and red blood cell extravasation in the lungs of NF-κB1[Δ/Δ] mice compared with WT mice (Figure 3c). In further support of these observations, an increased protein concentration was detected in the lung lavage fluid of urethane-treated NF-κB1[Δ/Δ] mice (Figure 3d). These data suggested that NF-κB1 protects lungs from urethane-induced pre-neoplastic injury.

One of the important roles of local inflammation and tissue damage is to establish a microenvironment that facilitates induction of oncogenic mutations and subsequent tumor initiation and progression. Thus, we compared the mutation frequency of the K-Ras oncogene in lung epithelium, an early event involved in lung tumorigenesis induced by urethane.[26] We found that about 6% of lung epithelial cells in urethane-treated WT mice
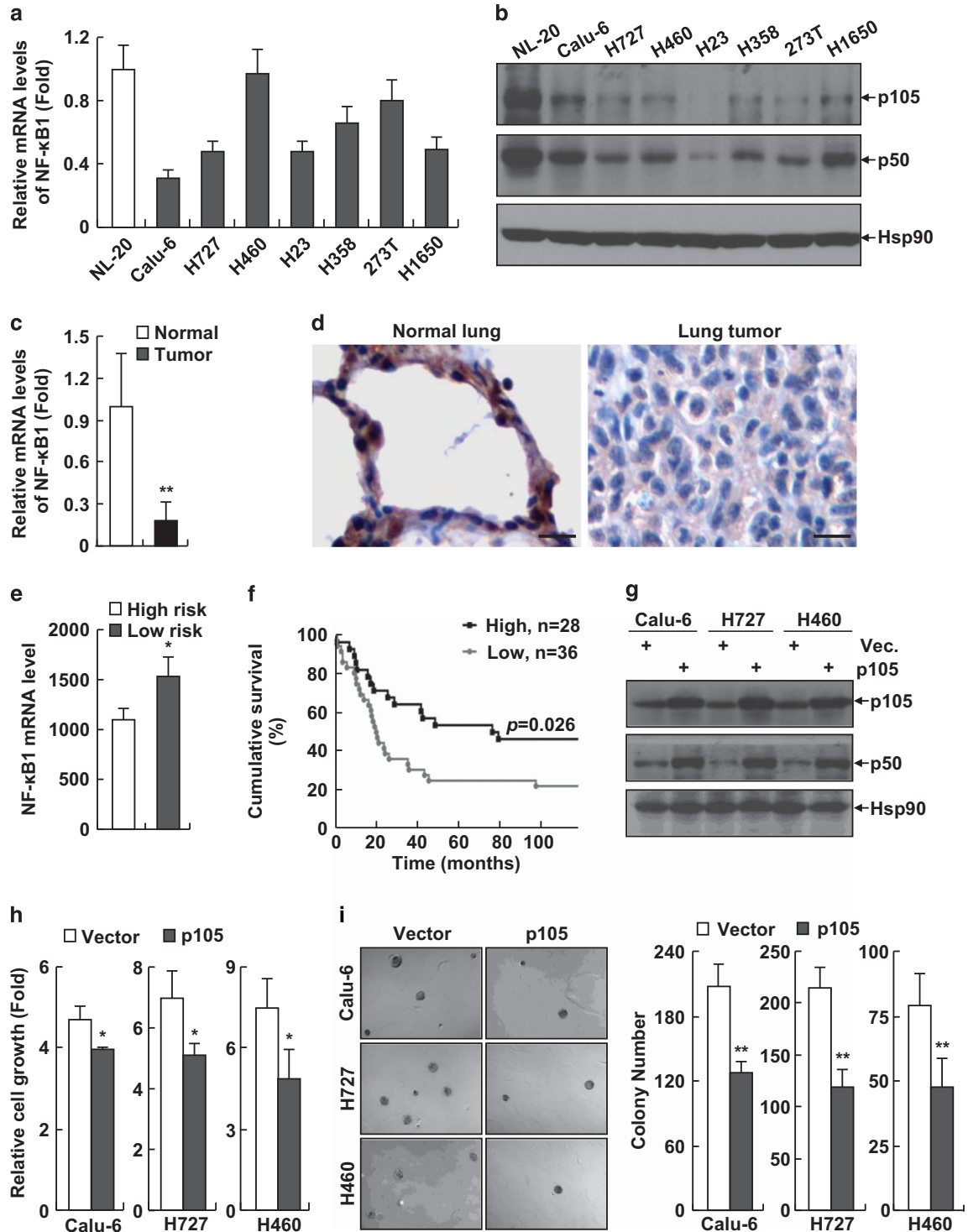
Figure 1. NF-κB1 expression is decreased in human lung cancer cells and its re-expression inhibits the tumorigenicities of human lung cancer cells. (**a**) Real-time PCR assays showing decreased expression of NF-κB1 mRNA in human lung cancer cell lines. Normal human lung epithelial cell line NL-20 was used as a control. Data shown are means ± s.d. ($n = 3$). (**b**) Immunoblotting (IB) assays showing decreased expression of NF-κB1 protein (p105 and p50) in human lung cancer cell lines. Hsp90 was used as a loading control. (**c**) Real-time PCR assays showing decreased expression of NF-κB1 mRNA in human primary lung tumor tissues. Normal control tissues from the same patients were used as controls. Data shown are means ± s.d. ($n = 10$; **$P < 0.01$). (**d**) IHC analysis showing decreased expression of NF-κB1 protein in human primary lung tumor tissues. Scale bar = 20 μm. (**e**) Gene array assays showing an association between downregulation of NF-κB1 mRNA and high risk of lung cancer in humans (the clinicopathological characteristics of patients used for the gene array were listed in the Supplementary Table S1). (**f**) Gene array assays showing an association between low NF-κB1 mRNA expression and poor survival of patients with lung cancer. (**g**) IB assays confirming the expression of p105 and p50 proteins in NF-κB1 human lung cancer stable cell lines. (**h**) Cell growth assays showing decreased growth rate of NF-κB1 human lung cancer stable cell lines. Cells were cultured 3 days before growth assays. Data shown are means ± s.d. ($n > 3$; *$P < 0.05$). (**i**) Soft agar colony-formation assays showing decreased anchorage-independent growth of NF-κB1 human lung cancer stable cell lines. Data shown are means ± s.d. ($n > 3$; **$P < 0.01$).
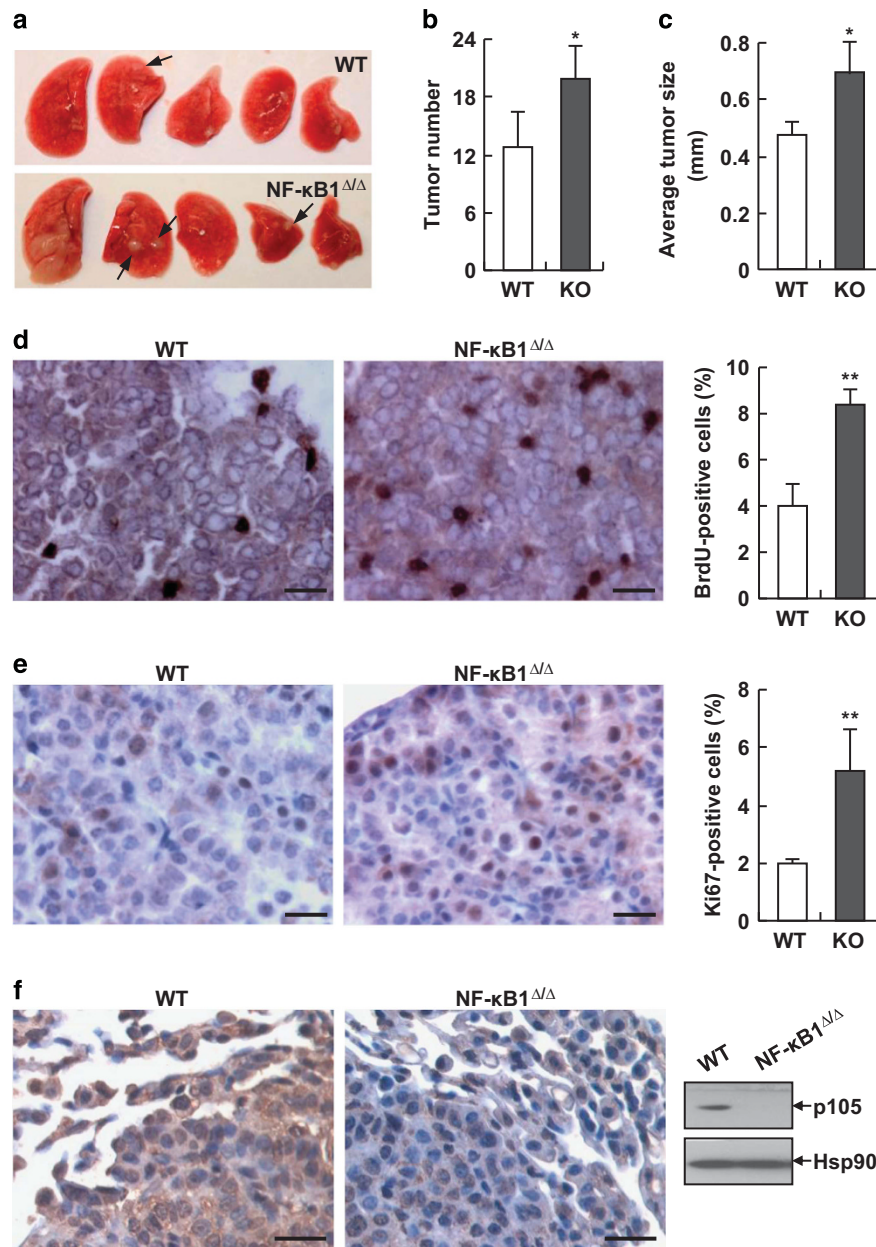
**Figure 2.** NF-κB1-knockout (NF-κB1$^{\Delta/\Delta}$) mice are more susceptible to urethane-induced lung tumorigenesis than WT mice. (**a**) Lung tissues from urethane-treated NF-κB1$^{\Delta/\Delta}$ mice and WT mice. Representative tumors are indicated by arrows. The large white nodules in the most left lung tissue of NF-kB1$^{\Delta/\Delta}$ mice are not tumors but actually damages associated with increased inflammation (see Figure 3). (**b**) Increased lung tumor multiplicities in urethane-treated NF-κB1$^{\Delta/\Delta}$ mice. Data shown are means ± s.d. ($n > 6$; *$P < 0.05$). (**c**) Increased average size of lung tumors in urethane-treated NF-κB1$^{\Delta/\Delta}$ mice. Data shown are means ± s.d. ($n > 5$; *$P < 0.05$). (**d**) BrdU labeling showing increased proliferation rate of lung tumors in urethane-treated NF-κB1$^{\Delta/\Delta}$ mice. Scale bar = 20 μm. BrdU-positive cells were also counted and represented as the percentage of total cells. Data shown are means ± s.d. ($n > 5$; **$P < 0.01$). (**e**) Ki-67 IHC staining showing increased proliferation rate of lung tumors in urethane-treated NF-κB1$^{\Delta/\Delta}$ mice. Scale bar = 20 μm. Ki-67-positive cells were also counted and represented as the percentage of total cells. Data shown are means ± s.d. ($n > 5$; **$P < 0.01$). (**f**) IHC staining and IB assays showing the absence of NF-κB1 proteins in lung tumors from urethane-treated NF-κB1$^{\Delta/\Delta}$ mice. Scale bar = 20 μm.

harbored K-Ras-activating mutations (Figure 3e). However, the same urethane treatment resulted in K-Ras mutations in over 10% of lung epithelial cells of NF-κB1$^{\Delta/\Delta}$ mice. Collectively, these data suggested that NF-κB1 prevents urethane-induced K-Ras oncogenic mutations and lung tumorigenesis through maintaining pulmonary homeostasis.

NF-κB1 suppresses lung cancers independent of its NF-κB activity
The human and mouse studies above clearly demonstrated a lung tumor-suppressive role for NF-κB1. Thus, it is both interesting and

important to determine the molecular mechanisms by which NF-κB1 suppresses lung cancer. First, we examined whether the tumor-suppressive role of NF-κB1 involves its NF-κB inhibition function, as its precursor form, p105, can act as an inhibitor of NF-κB through sequestering NF-κB in the cytoplasm.[1] Given the tumor-promoting role of RelA in lung and other cancers (Supplementary Figure S4), we examined its nuclear expression levels in murine NF-κB1$^{\Delta/\Delta}$ or WT lung tumors. However, those murine tumors showed no difference in the nuclear expression of RelA (Figure 4a). As a matter of fact, the immune cells surrounding
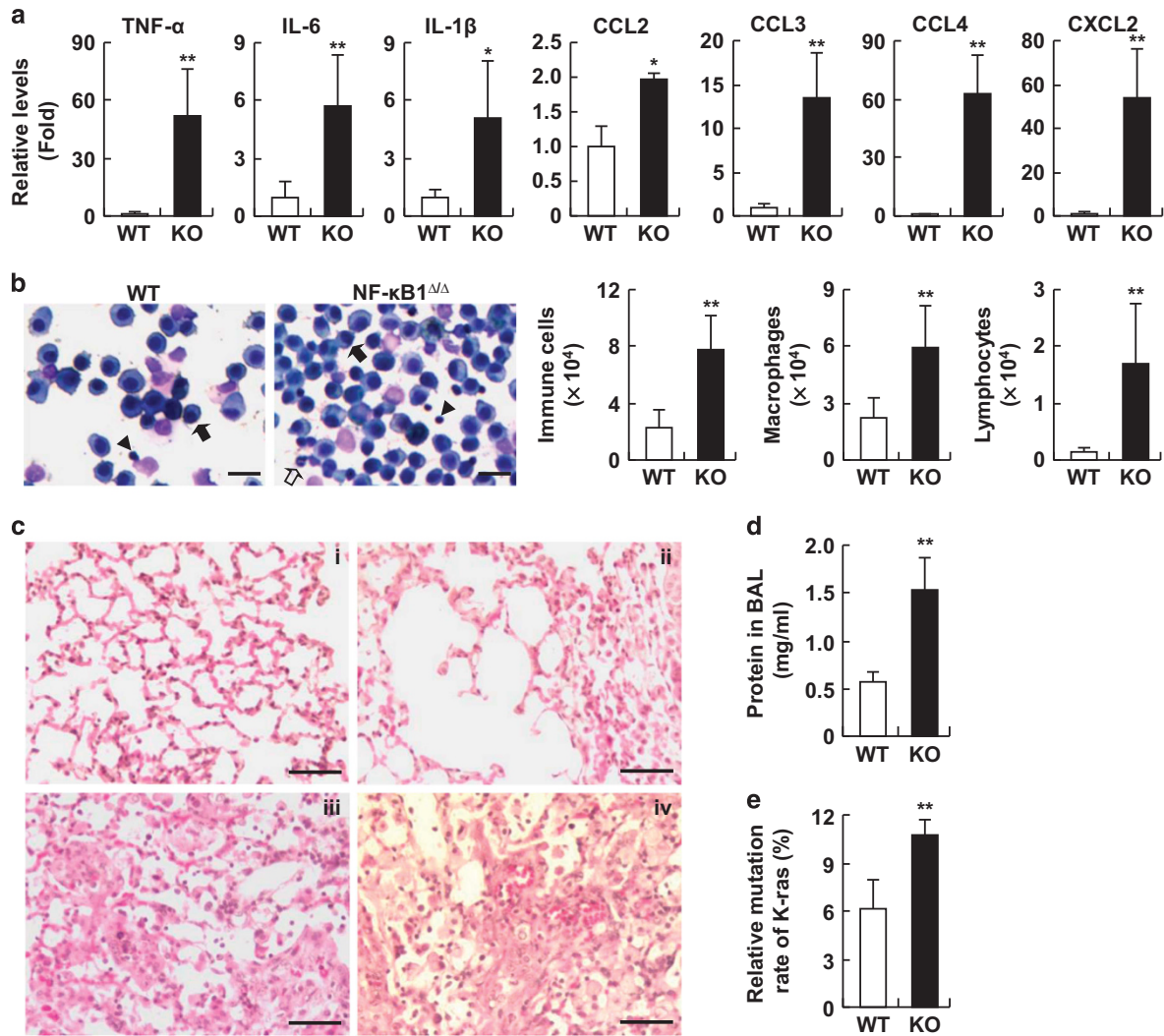
Figure 3. NF-κB1$^{\Delta/\Delta}$ mice are more susceptible to urethane-induced lung damage, pro-tumorigenic inflammation and K-Ras oncogenic mutation than WT mice. (**a**) Real-time PCR assays showing increased expressions of pro-inflammatory cytokines and chemokines in lungs of urethane-treated NF-κB1$^{\Delta/\Delta}$ mice. Data shown are means ± s.d. ($n > 5$; $*P < 0.05$; $**P < 0.01$). (**b**) Hema 3 staining assays showing increase in total immune cells, macrophages and lymphocytes, in BALF from urethane-treated NF-κB1$^{\Delta/\Delta}$ mice. Representative macrophages and neutrophils and lymphocytes were indicated by the filled arrows, open arrows and arrowheads, respectively. Scale bar = 20 μm. Data shown are means ± s.d. ($n > 5$; $**P < 0.01$). (**c**) Histological analysis showing severe lung injury in urethane-treated NF-κB1$^{\Delta/\Delta}$ mice. Minor histological changes in the lungs of urethane-treated WT mice (i). Severe epithelial cell death, protein leak, thickened alveoli, perivascular edema and hemorrhage in the lungs of urethane-treated NF-κB1$^{\Delta/\Delta}$ mice (ii–iv). Scale bar = 50 μm. (**d**) Bicinchoninic Acid (BCA) protein assay showing higher protein concentration in BALF from urethane-treated NF-κB1$^{\Delta/\Delta}$ mice. Data shown are means ± s.d. ($n = 5$; $**P < 0.01$). (**e**) Genomic sequencing showing increased K-Ras mutation frequency in the lungs of urethane-treated NF-κB1$^{\Delta/\Delta}$ mice. Data shown are means ± s.d. ($n = 4$; $**P < 0.01$).

or within the murine NF-κB1$^{\Delta/\Delta}$ or WT lung tumors also exhibited comparable expressions of nuclear RelA. Consistently, p105 re-expression had no obvious effect on RelA's nuclear expression in human NF-κB1^{low} lung cancer cells (Figure 4b). These data suggested that the tumor-suppressive role of NF-κB1 does not involve the NF-κB inhibitor function of p105.

Next, we examined whether the tumor-suppressive role of NF-κB1 is mediated by its mature form, p50. To do so, we stably expressed exogenous p50 to a level equal to the physiological level in human lung cancer cell lines in which endogenous NF-κB1 (both p105 and p50) is repressed (Figure 4c). As expected, re-expression of p50 did not affect the nuclear expression of RelA in those NF-κB1^{low} lung cancer cells (Figure 4c). In addition, p50 re-expression had no effect on the tumorigenicities of those cancer cells, as evidenced by our cell proliferation and soft-agar colony-formation assays (Figures 4d and e). Given our findings

that p105/p50 re-expression is sufficient to suppress the tumorigenicities of NF-κB1^{low} lung cancer cells (Figures 1g–i), these data together suggested that the lung tumor-suppressive role of NF-κB1 is mediated by its precursor form, p105, but independent of its NF-κB activities (p50 generation and p105 inhibition of NF-κB).

NF-κB1 p105 is required for the stabilization of the Tpl2 kinase in lung cancer cells

Previous studies suggested that p105, but not p50, is required for the stabilization of the Tpl2 kinase in murine macrophage under physiological conditions.[21] Thus, we examined the mRNA and protein expression levels of Tpl2 in NF-κB1$^{\Delta/\Delta}$ or WT lung tumors from urethane-treated mice. Although the mRNA expression levels of Tpl2 were comparable in these tumors, Tpl2 proteins could be detected only in WT tumors but not in NF-κB1$^{\Delta/\Delta}$ tumors
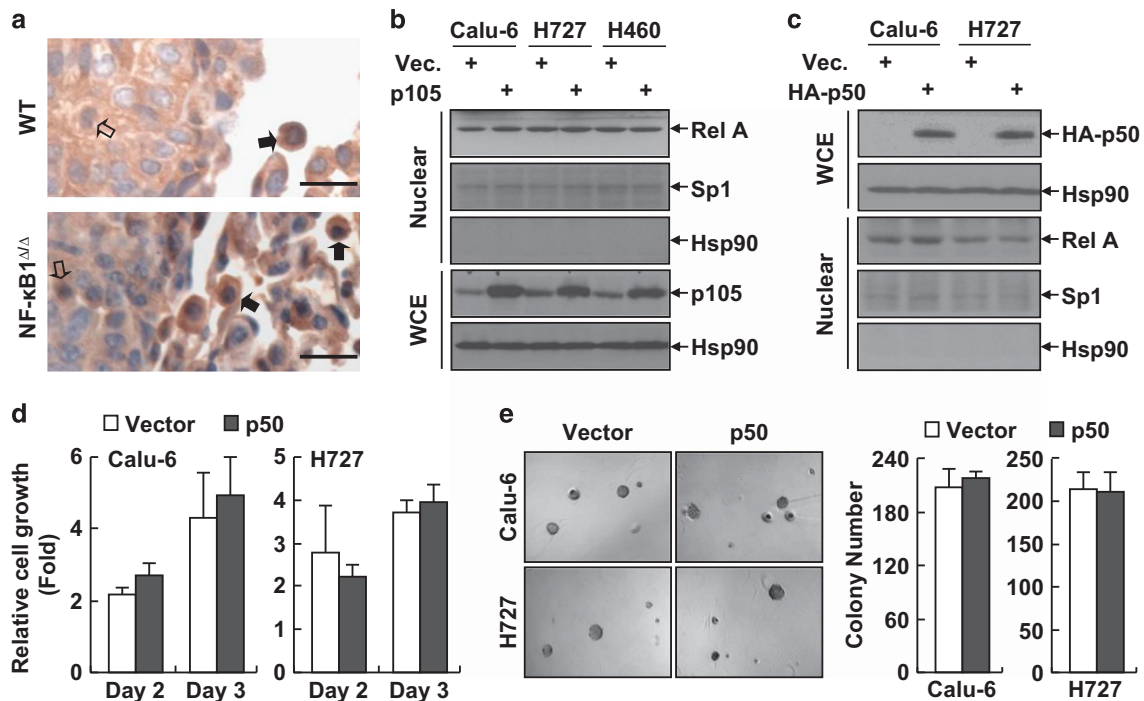
Figure 4. RelA activation in lung cancer cells is independent of NF-κB1 and expression of exogenous p50 has no effect on the tumorigenicities of NF-κB1[low] lung cancer cells. (**a**) IHC staining showing a similar RelA nuclear expression in NF-κB1[Δ/Δ] tumors and WT tumors from urethane-treated mice. Scale bar = 20 μm. Representatives of tumor cells and immune cells with positive staining of nuclear RelA are indicated by open and filled arrows, respectively. (**b**) Immunoblotting (IB) assays showing no change in RelA nuclear expression in p105 human lung cancer stable cell lines. (**c**) IB assays confirming expression of exogenous HA-tagged p50 in human lung cancer stable cell lines and showing no change in RelA nuclear expression in these stable cell lines. (**d**) Cell growth assays showing no change in the growth of p50 human lung cancer stable cell lines. Data shown are means ± s.d. ($n > 3$). (**e**) Soft agar colony-formation assays showing no change in anchorage-independent growth of p50 human lung cancer stable cell lines. Data shown are means ± s.d. ($n > 3$).

(Figures 5a and b). Similarly, we found that although there was no association between mRNA expression levels of NF-κB1 and Tpl2 (Supplementary Figure S5), their protein expression levels were highly associated with each other in human lung cancer cell lines (Figures 5c and d). These data suggested that NF-κB1 p105 is required for the protein stabilization of Tpl2 in both murine and human lung cancer cells.

To confirm the role of NF-κB1 p105 in Tpl2 stabilization in lung cancer cells, we checked whether p105 re-expression could re-store the expression of Tpl2 proteins in human NF-κB1[low] lung cancer cell lines. In this regard, we took advantage of human NF-κB1[low] lung cancer cell lines stably expressing p105, p50 or an empty vector, which had already been generated (see above Figures 1 and 4). As expected, re-expression of p105, but not p50, increased expression levels of endogenous Tpl2 proteins in human NF-κB1[low] lung cancer cell lines (Figure 5e), although both p105 and p50 did not affect the mRNA expression levels of Tpl2 in those same cells (Supplementary Figure S6). These data indicated that NF-κB1 p105 stabilizes Tpl2 protein in lung cancer cells.

Reconstitution of Tpl2 inhibits the tumorigenicities of NF-κB1[low] lung cancer cells

Although Tpl2 was originally identified as a proto-oncoprotein,[27,28] we examined whether p105 stabilization of Tpl2 protein accounts for the lung tumor-suppressive function of NF-κB1, as our recent studies demonstrate that STAT3 (signal transducer and activator of transcription 3), a well-known tumor promoter that is often referred as an oncoprotein, actually suppresses lung cancer initiation when specifically knocked out from lung epithelial cells.[29] In fact, a tumor-suppressive role of Tpl2 has been suggested in colon cancer and T-cell lymphoma

models.[30,31] Thus, we reconstituted Tpl2 into NF-κB1[low] lung cancer cells in which endogenous Tpl2 is disrupted due to p105 deficiency (Figure 6a). Consistent with the fact that Tpl2 functions as a downstream target of p105, Tpl2 reconstitution did not affect expression of p105 in those lung cancer cells (Figure 6a). However, interestingly enough, Tpl2 reconstitution blocked the growth in culture and colony formation in soft agar of those NF-κB1[low] lung cancer cells, exactly the same as p105 re-expression did (Figures 6b and c). On the other hand, knockdown of Tpl2 increased the growth of those cancer cells (Supplementary Figure S7). These data suggested that the lung tumor-suppressive function of NF-κB1 is attributed to p105 stabilization of Tpl2. These data also suggested a lung tumor-suppressive function for the Tpl2 proto-oncoprotein.

Tpl2-knockout mice resemble NF-κB1 knockouts in urethane-induced lung tumorigenesis

To further validate whether Tpl2 works downstream of NF-κB1 p105 in lung cancer suppression, we examined whether Tpl2-knockout (Tpl2[Δ/Δ]) mice, similar to NF-κB1 knockouts, are prone to urethane-induced lung tumorigenesis. Indeed, Tpl2[Δ/Δ]-knockout mice, similar to NF-κB1[Δ/Δ] mice, developed more and overall bigger lung tumors and have significant more atypical adenomatous hyperplasia, adenomas and adenocarcinomas in their lungs than WT mice after exposure to urethane (Figures 7a–c and Supplementary Figure S8). Moreover, Tpl2[Δ/Δ] tumors, similar to NF-κB1[Δ/Δ] ones, showed an increased cell proliferation rate (Figure 7d). In agreement with our human lung cancer cell line studies showing that Tpl2 did not affect NF-κB1 expression, Tpl2[Δ/Δ] tumors expressed a similar level of NF-κB1 proteins compared with WT tumors (Supplementary Figure S9). These data further
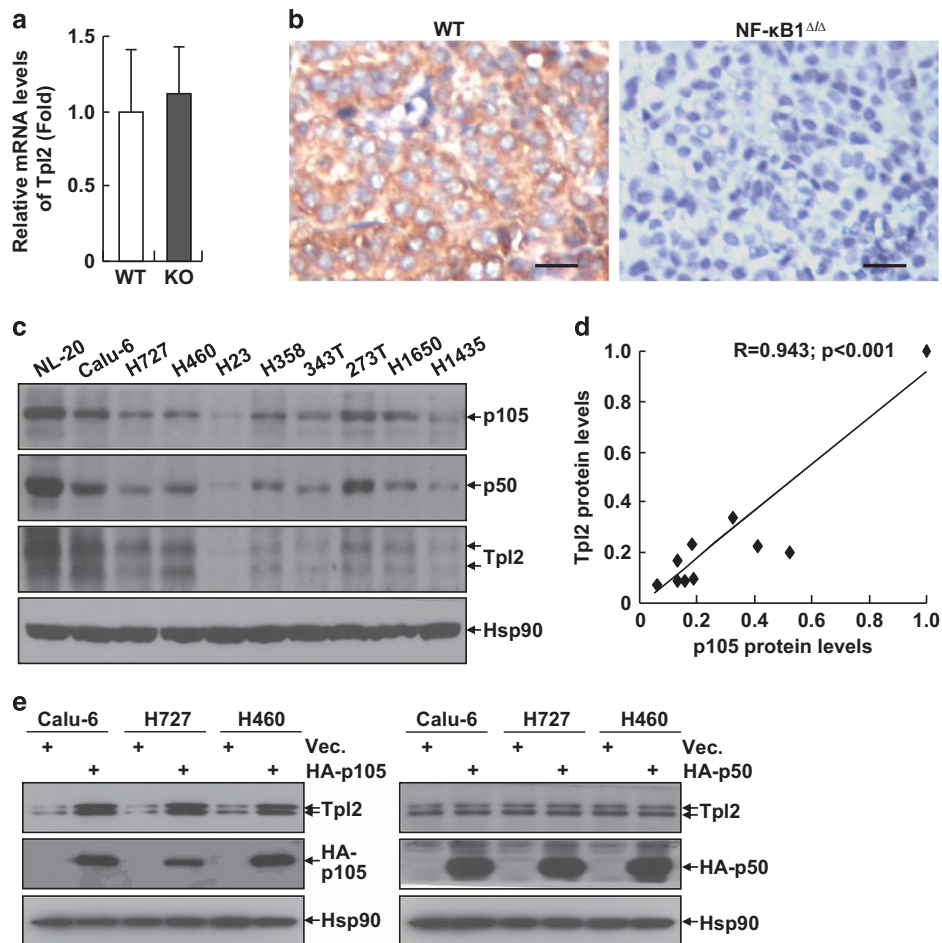
Figure 5. NF-κB1 p105 stabilizes Tpl2 in lung cancer cells. (**a**) Real-time PCR showing a similar expression level of Tpl2 mRNA in NF-κB1$^{\Delta/\Delta}$ tumors and WT tumors from urethane-treated mice. Data shown are means ± s.d. ($n > 3$). (**b**) IHC staining showing no Tpl2 protein in NF-κB1$^{\Delta/\Delta}$ tumors from urethane-treated mice. Scale bar = 20 μm. (**c**) IB assays showing the protein expression levels of p105, p50 and Tpl2 in human lung cancer cell lines. (**d**) Quantitation of IB assays in **c** showing a positive correlation in the protein expression levels of NF-κB1 and Tpl2 in human lung cancer cell lines. (**e**) IB assays showing restoration of Tpl2 protein expression in human lung cancer cell lines stably expressing HA-p105, but not HA-p50.

support that Tpl2 works downstream of p105 in suppressing lung cancer.

Remarkably, Tpl2$^{\Delta/\Delta}$ mice, similar to NF-κB1$^{\Delta/\Delta}$ mice, had a significantly elevated inflammation and injury in their lungs after exposure to urethane. The pro-inflammatory cytokine tumor necrosis factor-α and immune cell-attractive chemokine CCL2 were significantly increased in the lungs of Tpl2$^{\Delta/\Delta}$ mice compared with WT mice (Figure 7e). Consistently, more inflammatory cells, in particular macrophages and lymphocytes, were found in the BALF from Tpl2$^{\Delta/\Delta}$ mice (Figure 7f). Moreover, Tpl2$^{\Delta/\Delta}$ mice showed more severe lung damage, as evidenced by enhanced alveolar thickening and congestion, loss of integrity of the alveolar capillary membrane, air space enlargement, protein leak and red blood cell extravasation in their lungs (Figure 7g). These data clearly indicated that Tpl2$^{\Delta/\Delta}$ mice phenocopy NF-κB1 knockouts in urethane-induced lung tumorigenesis. All together, these studies strongly suggested that NF-κB1 restricts lung inflammation, maintains pulmonary homeostasis under oncogenic stress and suppresses lung tumorigenesis through p105 stabilization of Tpl2, but independent of its NF-κB-related activities.

DISCUSSION
Lung cancer accounts for ~ 1.2 million deaths annually worldwide and roughly 85% of the patients with lung cancer die of the

disease within 5 years.[9] A better understanding of the mechanisms underlying lung cancer development is desperately needed to design new effective therapies for this deadliest cancer. Recent studies suggest that NF-κB, in particular its prototypical member RelA, is involved in lung cancer development. RelA activation in lung cancer is associated with disease progression and poor patient survival.[12] On the other hand, genetic deletion of RelA significantly, although not completely, blocks lung tumorigenesis induced by the onogenic form of K-Ras in a mouse model.[16] Thus, RelA provides a novel target for lung cancer therapy. However, similar to other transcription factors, RelA is believed to be undruggable. Most currently available inhibitors of NF-κB indirectly target its upstream activating kinase IKK, which activates not only RelA but also all other members of the NF-κB family, including NF-κB1, another prototypical NF-κB member and most important functional partner of RelA.[1,32] Given the functional complex of NF-κB, it is thus paramount important and interesting to delineate the role of NF-κB1 and other NF-κB members in lung cancer.

Astonishingly, both animal and human studies showed that in sharp contrast to RelA, NF-κB1 actually suppresses lung tumorigenesis. Genetic deletion of NF-κB1 makes animals more sensitive to lung cancer induction. Compared with WT mice, NF-κB1-deficient mice developed much more and larger lung tumors after the same treatment of the smoke carcinogen

urethane (Figure 2). Similarly, the expression of NF-κB1 is repressed in human lung cancer cell lines and primary tissues, and low expression of NF-κB1 is associated with high risk of lung cancer in humans and poor patient survival (Figure 1). More importantly, NF-κB1 re-expression in those lung cancer cells inhibits their tumorigenicity (Figure 1). These data indicate that NF-κB1 suppresses both initiation and progression of lung cancer. Of note, this is the first evidence directly showing a tumor-suppressive role for a prototypical NF-κB member.

Remarkably, the lung tumor-suppressive function of NF-κB1 is independent of its two NF-κB-related activities: generation of p50 and NF-κB inhibition by p105. As a matter of fact, the two NF-κB-related activities of NF-κB1 have a minor, if any, role in NF-κB activation in lung cancer cells. Although p105 re-expression reverses the tumor phenotypes of NF-κB1^{low} lung cancer cells (Figure 1), it fails to block persistent RelA activation in those malignant cells (Figure 4), suggesting that p105 does not exhibit NF-κB inhibitor function in lung cancer cells. Conversely, p50

re-expression has no effect on the tumorigenicity of NF-κB1^{low} lung cancer cells (Figure 4). This is the first evidence showing that NF-κB1 p50 is dispensable for cancer development. It also suggests that RelA can exert tumor-promoting role in the absence of its most important functional partner, p50. Collectively, these findings significantly improve our understanding of the complex function of NF-κB and further suggest that NF-κB1 exerts its tumor-suppressive role in lung cancer via NF-κB-independent function of p105.

Our mechanistic studies indicate that p105 suppresses lung cancer initiation and progression through stabilization of the Tpl2 kinase. Human and mouse lung cancers defective in NF-κB1 are also defective in the expression of Tpl2 protein (Figure 5). Re-expression of p105, but not p50, restores Tpl2 protein expression in those NF-κB1^{low} lung cancer cells, although both p105 and p50 do not affect the RNA expression level of Tpl2. More importantly, re-expression of Tpl2, similar to re-expression of p105, inhibits the tumorigenicity of NF-κB1^{low} lung cancer cells (Figure 1
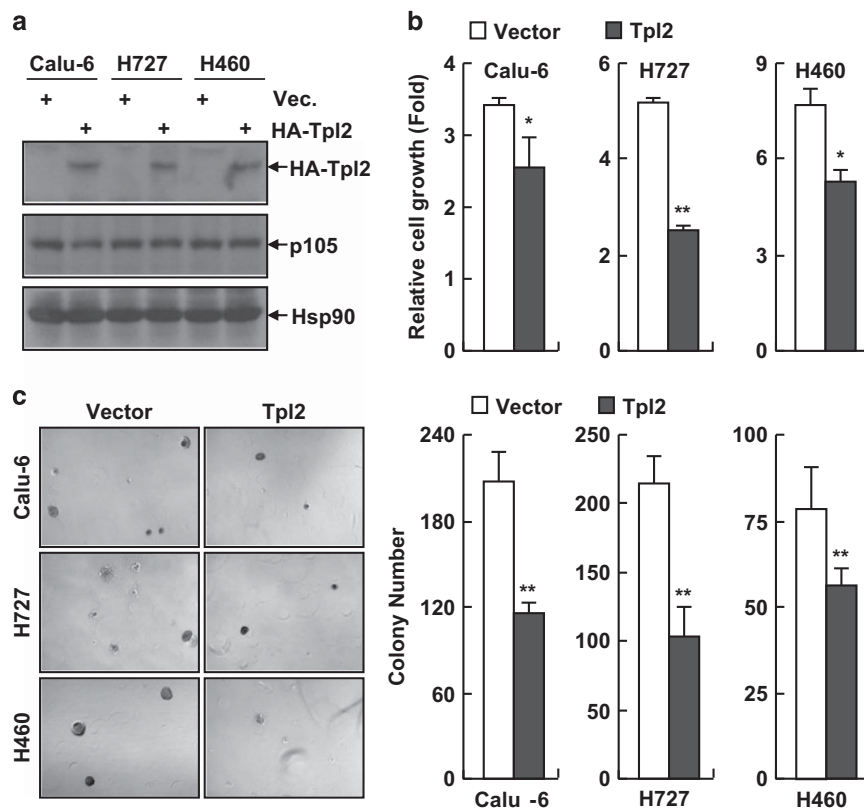
Figure 6. Tpl2 expression blocks the tumorigenicities of human NF-κB1^{low} lung cancer cells. (**a**) Immunoblotting (IB) assays confirming the expression of exogenous HA-tagged Tpl2 in human lung cancer stable cell lines. (**b**) Cell growth assays showing decreased growth rate of Tpl2 human lung cancer stable cell lines. Cells were cultured 3 days before growth assays. Data shown are means ± s.d. ($n > 3$; *$P < 0.05$; **$P < 0.01$). (**c**) Soft agar colony-formation assays showing decreased anchorage-independent growth of Tpl2 human lung cancer stable cell lines. Data shown are means ± s.d. ($n > 3$; **$P < 0.01$).

Figure 7. Tpl2-knockout (Tpl2$^{Δ/Δ}$) mice are more susceptible to urethane-induced lung damage, pro-tumorigenic inflammation and tumorigenesis than WT mice. (**a**) Lung tissues from urethane-treated Tpl2$^{Δ/Δ}$ mice and WT mice. Representative tumors are indicated by arrows. (**b**) Increased lung tumor multiplicities in urethane-treated Tpl2$^{Δ/Δ}$ mice. Data shown are means ± s.d. ($n > 6$; *$P < 0.05$). (**c**) Increased average size of lung tumors in urethane-treated Tpl2$^{Δ/Δ}$ mice. Data shown are means ± s.d. ($n > 5$; *$P < 0.05$). (**d**) BrdU labeling showing increased proliferation rate of lung tumors in urethane-treated Tpl2$^{Δ/Δ}$ mice. Scale bar = 20 μm. BrdU-positive cells were also counted and represented as the percentage of total cells. Data shown are means ± s.d. ($n > 5$; **$P < 0.01$). (**e**) Real-time PCR assays showing increased expressions of tumor necrosis factor-α (TNF-α) and CCL2 in the lungs of urethane-treated Tpl2$^{Δ/Δ}$ mice. Data shown are means ± s.d. ($n > 5$; *$P < 0.05$). (**f**) Hema 3 staining assays indicating increase in macrophages and lymphocytes in BALF from urethane-treated Tpl2$^{Δ/Δ}$ mice. Data shown are means ± s.d. ($n > 5$; **$P < 0.01$). (**g**) Histological analysis showing severe lung injury in urethane-treated Tpl2$^{Δ/Δ}$ mice. Severe epithelial cell death, protein leak, thickened alveoli, perivascular edema and hemorrhage in the lungs of urethane-treated Tpl2$^{Δ/Δ}$ mice were shown. Scale bar = 50 μm. (i) WT mice; (ii–iv) Tpl2$^{Δ/Δ}$ mice.
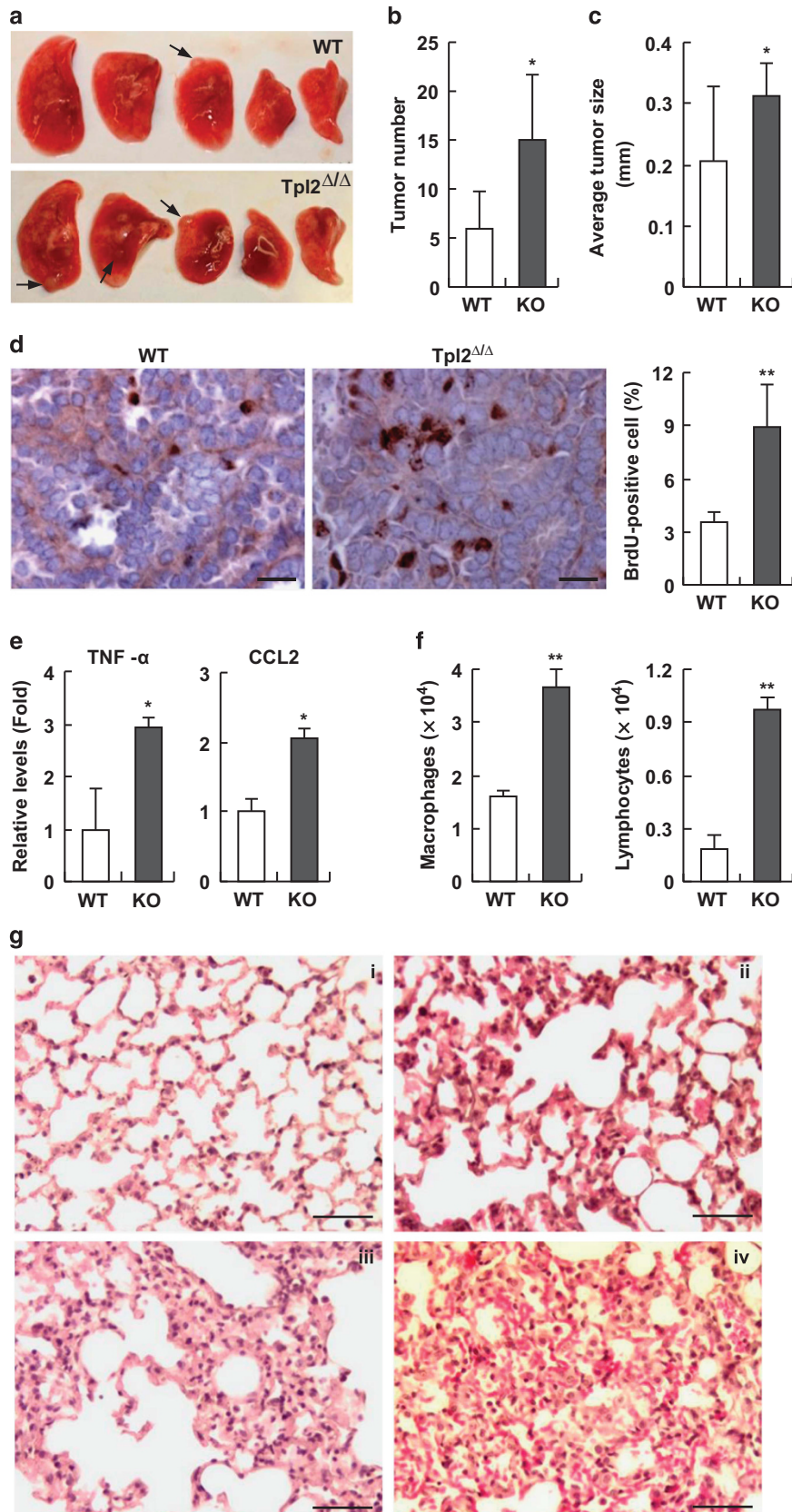
versus Figure 6) and Tpl2-knockout mice faithfully recapitulate NF-κB1 knockouts in urethane-induced lung tumorigenesis (Figures 2 and 3 versus Figure 7).

Interestingly, our studies suggest that the lung tumor-suppressive functions of the noncanonical p105/Tpl2 signaling pathway involve its different abilities in regulating the growth of normal and malignant lung cells. It suppresses lung cancer induction through maintaining lung epithelial survival and homeostasis under inflammatory and oncogenic stress, whereas it inhibits lung cancer progression via blocking cancer cell growth (Figures 1–7). In addition, the p105/Tpl2 signaling pathway also suppresses activation of immune cells, in particular macrophages and lymphocytes, restricting inflammation under oncogenic stress. In association with an increase in the incidence and size of lung cancer, p105- or Tpl2-knockout mice display an increased pulmonary inflammation and injury in response to urethane (Figures 2, 3 and 7). Lung damage and inflammation enhance each other and facilitate K-Ras-activating mutations (Figure 3). Activated K-Ras in turn induces and exacerbates lung inflammation and damage (Figure 3). In this way, lung damage, inflammation and K-Ras mutations function as extrinsic and/or intrinsic forces driving lung cancer initiation and progression. Loss of p105/Tpl2 signaling in cancer cells also directly contributes to lung cancer growth. It seems that the intrinsic p105/Tpl2 signaling pathway within lung cancer cells activates the mitogen-activated protein kinase kinase 7 to activate the c-Jun N-terminal kinase, which in turn induces the activation of the tumor suppressor p53, resulting in proliferation inhibition and apoptosis induction of cancer cells.[33,34] In support of this, lung cancer cells defective in p105 or Tpl2 have higher proliferation rates and re-expression of p105 or Tpl2 suppresses growth of those lung cancer cells (Figures 1 and 6).

In summary, the data presented here demonstrate that in contrast to the tumor-promoting role of RelA, NF-κB1 suppresses lung cancer development and progression. The tumor-suppressive function of NF-κB1 is mediated by p105 stabilization of Tpl2, but independent of its NF-κB function. On one hand, the noncanonical p105/Tpl2 signaling pathway contributes to lung cell survival and pulmonary homeostasis under inflammation and oncogenic stress, therefore suppressing lung tumorigenesis. On the other hand, the p105/Tpl2 signaling pathway within lung cancer cells directly inhibits cancer cell growth. Moreover, the p105/Tpl2 signaling pathway also limits immune cell activation and restricts pulmonary inflammation under oncogenic stress. These findings describe a previously unidentified role of the p105/Tpl2 signaling pathway in lung cancer suppression and, therefore, significantly improve our understanding of this deadliest human cancer. These findings also help us understand the complex functions of NF-κB.

MATERIALS AND METHODS

Illumina microarray analysis
The gene array assay was performed essentially as previously described.[35] Briefly, total RNAs were extracted from formalin-fixed paraffin-embedded human lung cancer tissues. The integrity of the RNAs was examined by using the Agilent platform (2100 Bioanalyzer; Agilent Technologies, Palo Alto, CA, USA). High-quality total RNA was labeled using Illumina TotalPrep RNA Amplification kit from Ambion (Grand Island, NY, USA) and hybridized on the Illumina Whole-Genome DASL Assay (HT-12 V4 Bead Chip platform, San Diego, CA, USA) according to the manufacturer's instructions. The studies were approved by the University of Pittsburgh Institutional Review Board.

Animals
NF-κB1$^{\Delta/\Delta}$ mice and Tpl2$^{\Delta/\Delta}$ mice under C57BL/6 background were from Jackson Laboratory (Bar Harbor, ME, USA) and Dr Philip N Tsichlis (Tufts University, Boston, MA, USA). As C57BL/6 mice are resistant to urethane-induced lung tumorigenesis,[15] those mice were backcrossed to

WT FVB/N mice (Jackson Laboratory) for more than 10 generations, for pure FVB/N background. All animals were housed under specific pathogen-free conditions at the Hillman Cancer Center of the University of Pittsburgh Cancer Institute. Animal experiments were approved by the Institutional Animal Care and Use Committee of the University of Pittsburgh.

Lung carcinogenesis
For urethane induction of lung tumors, 6- to 8-week-old NF-κB1$^{\Delta/\Delta}$ mice, Tpl2$^{\Delta/\Delta}$ mice or WT FVB/N mice were intraperitoneally injected with urethane (1 mg/g body weight, Sigma-Aldrich, St Louis, MO, USA) one time per week for 6 weeks. Six weeks post-urethane treatment, all mice were killed for lung tumor examinations.

Bronchioalveolar lavage
Mice were killed and their lungs were lavaged three times with phosphate-buffered saline. The recovered BALFs were centrifuged. Cells from BALF were visualized by Hema3-staining. BALF total cell counts were determined by using a grid hemocytometer and numbers of different leukocytes were obtained by counting at least 400 cells on Hema3-stained cytocentrifuge slides. Supernatants of BALF were subjected to the Bicinchoninic Acid protein assay (Thermo Scientific, Rockford, IL, USA) for protein quantitation.

Lung tumor enumeration
Surface tumors in mouse lungs were counted by three blinded readers under a dissecting microscope. Tumor diameters were determined by microcalipers.

Histology and IHC
Mouse and human lung tissues were fixed in formalin, embedded in paraffin and cut into 5-μm-thick sections. Sections were stained with hematoxylin and eosin or subjected to IHC as previously described.[29,36] The following primary antibodies were used: anti-p105/50 (ab32360) (Abcam, Cambridge, MA, USA), anti-Tpl2 (sc-720) and anti-Ki-67 (sc-7846) (Santa Cruz Biotechnology, Dallas, TX, USA).

BrdU labeling
Mice were intraperitoneally injected with 50 mg/kg BrdU (Sigma-Aldrich) 24 h before killing. Mouse lung tissue sections were stained with anti-BrdU (Sigma-Aldrich). More than 3000 cells per lung were counted in randomly selected fields. BrdU labeling index was calculated as the percentage of labeled cells per total cells counted as described previously.[37]

Quantitative PCR analysis
Mouse lung tissues, BAL cells or type II epithelial cells were subjected to RNA extraction, RNA reverse transcription and real-time PCR as described.[28–40] The expression levels of the indicated genes were normalized to that of ribosomal 18S within the same cells. Primer pairs used for quantitative PCR are listed in the Supplementary Table S2.

Isolation of lung type II epithelial cells
The detailed protocol has been described before.[29] Briefly, crude lung cell suspensions were prepared by intratracheal instillation of Dispase and agarose followed by mechanical disaggregation of the lungs. Crude cell suspensions were purified by negative selection using a biotinylated-antibody, streptavidin-coated biomagnetic particle system. Cell purities were determined by Pap staining and confirmed ultrastructurally. Purified ATII cells were cultured on fibronectin-coated chamber slides and maintained for up to 5 days in Dulbecco's modified Eagle's medium with 10% fetal bovine serum.

K-Ras sequencing
The exon 3 of the K-Ras gene was amplified by PCR using AccuPrime Pfx polymerase (Invitrogen, Grand Island, NY, USA) for DNA sequencing. The mutation frequencies of K-Ras in type II lung epithelial cells were determined by the ratios of the area of the mutated nucleotide versus that of WT nucleotide of K-Ras in the sequencing map as described before.[29]

Retroviral transduction and generation of stable cDNA transfectants

All the experiments involving virus were performed under Biohazard Safety Level BSL 2+ conditions. HEK293T cells were transfected with the green fluorescent protein-expressing retroviral vector pCLXSN(GFP) alone or vector simultaneously expressing p105, p50 or Tpl2 using FuGENE 6 (Roche Applied Science, Indianapolis, IN, USA) followed by viral supernatant collection and infection of human lung cancer cell lines as described.[41] Stable transfectants were obtained by green fluorescent protein sorting.

Colony-formation assays

Soft agar assays were performed as previously described.[42] Briefly, cell suspensions in culture medium containing 0.6% SeaPlaque (Cambrex BioScience, Rockland, ME, USA) low-melting agarose were plated on the top of 1% agarose in culture medium. Colony growth was scored after 21 days of cell incubation. All the colony-formation assays presented in this study were repeated in at least three independent experiments.

Immunoblotting analysis

Whole-cell extracts were prepared by lysing cells in radioimmune precipitation assay buffer (50 mM Tris-HCl, pH 7.4, 150 mM NaCl, 1 mM EDTA, 0.25% (w/v) sodium deoxycholate, 1% (v/v) Nonidet P-40, 1 mM dithiothreitol) supplemented with 1 mM phenylmethylsulfonyl fluoride. Cell nuclear extracts were prepared using hypertonic buffer (20 mM HEPES, pH 8.0, 1 mM EDTA, 20% (v/v) glycerol, 0.1% (v/v) Triton X-100 and 400 mM NaCl) after the cytoplasmic fraction was extracted by the hypotonic buffer (20 mM HEPES, pH 8.0, 10 mM KCl, 1 mM MgCl$_2$, 0.1% (v/v) Triton X-100 and 20% (v/v) glycerol). The purity of the nuclear fractions was confirmed by detecting expression of Sp1 (nuclear marker), but not Hsp90 (cytoplasm marker). The whole-cell lysates and nuclear extracts were subjected to SDS–polyacrylamide gel electrophoresis and immunoblotting using the indicated antibodies as described previously.[43]

Statistical analysis

Data were reported as mean ± s.d. The Student's t-test (two tailed) was used to assess significance of differences between two groups and P-values < 0.05 and 0.01 were considered statistically significant and highly statistically significant, respectively.[44] Log-rank tests were used to compare overall survival between high and low NF-κB1 expression.[45]

CONFLICT OF INTEREST

The authors declare no conflict of interest.

REFERENCES

1 Fu J, Xiao G. NF-κB and cancer: a paradigm of yin-yang. *Am J Cancer Res* 2011; **1**: 192–221.

2 Gilmore TD. The Rel/NF-κB/IκB signal transduction pathway and cancer. *Cancer Treat Res* 2003; **115**: 241–265.

3 Karin M, Greten FR. NF-κB: linking inflammation and immunity to cancer development and progression. *Nat Rev Immunol* 2005; **5**: 749–759.

4 Xiao G, Rabson AB, Young W, Qing G, Qu Z. Alternative pathways of NF-κB activation: a double-edged sword in health and disease. *Cytokine Growth Factor Rev* 2006; **17**: 281–293.

5 Rayet B, Gélinas C. Aberrant rel/nfκb genes and activity in human cancer. *Oncogene* 1999; **18**: 6938–6947.

6 Wong KK, Jacks T, Dranoff G. NF-κB fans the flames of lung carcinogenesis. *Cancer Prev Res (Phila)* 2010; **3**: 403–405.

7 Cai Z, Tchou-Wong KM, Rom WN. NF-κB in lung tumorigenesis. *Cancers (Basel)* 2011; **3**: 4258–4268.

8 Chen W, Li Z, Bai L, Lin Y. NF-κB in lung cancer, a carcinogenesis mediator and a prevention and therapy target. *Front Biosci (Landmark Ed)* 2011; **16**: 1172–1185.

9 Siegel R, Ma J, Zou Z, Jemal A. Cancer statistics, 2014. *CA Cancer J Clin* 2014; **64**: 9–29.

10 Wen J, Fu JH, Zhang W, Guo M. Lung carcinoma signaling pathways activated by smoking. *Chin J Cancer* 2011; **30**: 551–558.

11 Hecht SS. Cigarette smoking and lung cancer: chemical mechanisms and approaches to prevention. *Lancet Oncol* 2002; **3**: 461–469.

12 Zhang D, Jin X, Wang F, Wang S, Deng C, Gao Z et al. Combined prognostic value of both RelA and IκB-α expression in human non-small cell lung cancer. *Ann Surg Oncol* 2007; **14**: 3581–3592.

13 Bassères DS, Ebbs A, Cogswell PC, Baldwin AS. IKK is a therapeutic target in KRAS-Induced lung cancer with disrupted p53 activity. *Genes Cancer* 2014; **5**: 41–55.

14 Meylan E, Dooley AL, Feldser DM, Shen L, Turk E, Ouyang C et al. Requirement for NF-κB signaling in a mouse model of lung adenocarcinoma. *Nature* 2009; **462**: 104–107.

15 Stathopoulos GT, Sherrill TP, Cheng DS, Scoggins RM, Han W, Polosukhin VV et al. Epithelial NF-κB activation promotes urethane-induced lung carcinogenesis. *Proc Natl Acad Sci USA* 2007; **104**: 18514–18519.

16 Bassères DS, Ebbs A, Levantini E, Baldwin AS. Requirement of the NF-κB subunit p65/RelA for K-Ras-induced lung tumorigenesis. *Cancer Res* 2010; **70**: 3537–3546.

17 Jones DR, Broad RM, Madrid LV, Baldwin Jr AS, Mayo MW. Inhibition of NF-κB sensitizes non-small cell lung cancer cells to chemotherapy-induced apoptosis. *Ann Thorac Surg* 2000; **70**: 930–936.

18 Chariot A. The NF-κB-independent functions of IKK subunits in immunity and cancer. *Trends Cell Biol* 2009; **19**: 404–413.

19 Mulero MC, Ferres-Marco D, Islam A, Margalef P, Pecoraro M, Toll A et al. Chromatin-bound IκBα regulates a subset of polycomb target genes in differentiation and cancer. *Cancer Cell* 2013; **24**: 151–166.

20 Belich MP, Salmerón A, Johnston LH, Ley SC. TPL-2 kinase regulates the proteolysis of the NF-κB-inhibitory protein NF-κB1 p105. *Nature* 1999; **397**: 363–368.

21 Waterfield MR, Zhang M, Norman LP, Sun SC. NF-κB1/p105 regulates lipopolysaccharide-stimulated MAP kinase signaling by governing the stability and function of the Tpl2 kinase. *Mol Cell* 2003; **11**: 685–694.

22 Tuveson DA, Jacks T. Modeling human lung cancer in mice: similarities and shortcomings. *Oncogene* 1999; **18**: 5318–5324.

23 Sha WC, Liou HC, Tuomanen EI, Baltimore D. Targeted disruption of the p50 subunit of NF-κB leads to multifocal defects in immune responses. *Cell* 1995; **80**: 321–330.

24 Dougan M, Li D, Neuberg D, Mihm M, Googe P, Wong KK et al. A dual role for the immune response in a mouse model of inflammation-associated lung cancer. *J Clin Invest* 2011; **121**: 2436–2446.

25 Qu Z, Sun F, Zhou J, Li L, Shapiro SD, Xiao G. Interleukin-6 prevents the initiation but enhances the progression of lung cancer. *Cancer Res* 2015; e-pub ahead of print 29 June 2015.

26 Ichikawa T, Yano Y, Uchida M, Otani S, Hagiwara K, Yano T. The activation of K-ras gene at an early stage of lung tumorigenesis in mice. *Cancer Lett* 1996; **107**: 165–170.

27 Aoki M, Akiyama T, Miyoshi J, Toyoshima K. Identification and characterization of protein products of the cot oncogene with serine kinase activity. *Oncogene* 1991; **6**: 1515–1519.

28 Patriotis C, Makris A, Bear SE, Tsichlis PN. Tumor progression locus 2 (Tpl-2) encodes a protein kinase involved in the progression of rodent T-cell lymphomas and in T-cell activation. *Proc Natl Acad Sci USA* 1993; **90**: 2251–2255.

29 Zhou J, Qu Z, Yan S, Sun F, Whitsett JA, Shapiro SD et al. Differential roles of STAT3 in the initiation and growth of lung cancer. *Oncogene* 2014; **34**: 3804–3814.

30 Serebrennikova OB, Tsatsanis C, Mao C, Gounaris E, Ren W, Siracusa LD et al. Tpl2 ablation promotes intestinal inflammation and tumorigenesis in Apcmin mice by inhibiting IL-10 secretion and regulatory T-cell generation. *Proc Natl Acad Sci USA* 2012; **109**: E1082–E1091.

31 Tsatsanis C, Vaporidi K, Zacharioudaki V, Androulidaki A, Sykulev Y, Margioris AN et al. Tpl2 and ERK transduce antiproliferative T cell receptor signals and inhibit transformation of chronically stimulated T cells. *Proc Natl Acad Sci USA* 2008; **105**: 2987–2992.

32 Gilmore TD, Herscovitch M. Inhibitors of NF-κB signaling: 785 and counting. *Oncogene* 2006; **25**: 6887–6899.

33 Gkirtzimanaki K, Gkouskou KK, Oleksiewicz U, Nikolaidis G, Vyrla D, Liontos M et al. TPL2 kinase is a suppressor of lung carcinogenesis. *Proc Natl Acad Sci USA* 2013; **110**: E1470–E1479.

34 Schramek D, Kotsinas A, Meixner A, Wada T, Elling U, Pospisilik JA et al. The stress kinase MKK7 couples oncogenic stress to p53 stability and tumor suppression. *Nat Genet* 2011; **43**: 212–219.

2310

35 Qing G, Qu Z, Xiao G. Endoproteolytic processing of C-terminally truncated NF-κB2 precursors at κB-containing promoters. *Proc Natl Acad Sci USA* 2007; **104**: 5324–5329.

36 Sun F, Xiao Y, Qu Z. Oncovirus KSHV represses tumor suppressor PDLIM2 to persistently activate NF-κB and STAT3 transcription factors for tumorigenesis and tumor maintenance. *J Biol Chem* 2015; **290**: 7362–7368.

37 Qu Z, Sun D, Young W. Lithium promotes neural precursor cell proliferation: evidence for the involvement of the non-canonical GSK-3β-NF-AT signaling. *Cell Biosci* 2011; **1**: 18.

38 Qu Z, Fu J, Ma H, Zhou J, Jin M, Mapara MY et al. PDLIM2 restricts Th1 and Th17 differentiation and prevents autoimmune disease. *Cell Biosci* 2012; **2**: 23.

39 Yan P, Fu J, Qu Z, Li S, Tanaka T, Grusby MJ et al. PDLIM2 suppresses HTLV-I Tax-mediated tumorigenesis by targeting Tax into the nuclear matrix for proteasomal degradation. *Blood* 2009; **113**: 4370–4380.

40 Fu J, Qu Z, Yan P, Ishikawa C, Aqeilan RI, Rabson AB et al. The tumor suppressor gene WWOX links the canonical and noncanonical NF-κB pathways in HTLV-I Tax-mediated tumorigenesis. *Blood* 2011; **117**: 1652–1661.

41 Fu J, Yan P, Li S, Qu Z, Xiao G. Molecular determinants of PDLIM2 in suppressing HTLV-I Tax-mediated tumorigenesis. *Onocogene* 2010; **29**: 6499–6507.

42 Qu Z, Yan P, Fu J, Jiang J, Grusby MJ, Smithgall TE et al. DNA methylation-dependent repression of PDLIM2 in colon cancer and its role as a potential therapeutic target. *Cancer Res* 2010; **70**: 1766–1772.

43 Qing G, Qu Z, Xiao G. Stabilization of basally translated NF-κB-inducing kinase (NIK) protein functions as a molecular switch of processing of NF-κB2 p100. *J Biol Chem* 2005; **280**: 40578–40582.

44 Qu Z, Fu J, Yan P, Hu J, Cheng SY, Xiao G. Epigenetic repression of PDLIM2: implications for the biology and treatment of breast cancer. *J Biol Chem* 2010; **285**: 11786–11792.

45 Stabile LP, Dacic S, Land SR, Lenzner DE, Dhir R, Acquafondata M et al. Combined analysis of estrogen receptor beta-1 and progesterone receptor expression identifies lung cancer patients with poor outcome. *Clin Cancer Res.* 2011; **17**: 154–164.

Supplementary Information accompanies this paper on the Oncogene website (http://www.nature.com/onc)